

## Step bunching caused by annealing vicinal GaAs(001) in AsH<sub>3</sub> and hydrogen ambient in its stationary state

K. Hata\* and H. Shigekawa

*Institute of Materials Science and Center for Tsukuba Advanced Research Alliance, University of Tsukuba, Tsukuba 305, Japan*

T. Ueda and M. Akiyama

*OKI Semiconductor Technology Company Ltd., 550-5 Higashi-Asakawa, Hachioji, Tokyo 193, Japan*

T. Okano

*Institute of Industrial Science, The University of Tokyo, 7-22-1 Roppongi, Minato-ku, Tokyo 106, Japan*

(Received 11 April 1997; revised manuscript received 8 September 1997)

The growth of step bunches on vicinal GaAs(001) annealed in AsH<sub>3</sub>/H<sub>2</sub> ambient stops after the step bunches reach a particular size. The surface has reached a stationary state with the AsH<sub>3</sub>/H<sub>2</sub> ambient. In this paper, we report how the surface morphology of step bunches in the stationary state depends on the annealing conditions. The fact that step bunching always occurred when vicinal GaAs(001) substrates were annealed in AsH<sub>3</sub>/H<sub>2</sub> ambient led us to conclude that AsH<sub>3</sub>/H<sub>2</sub> is directly related to its cause. In order to understand the formation mechanism of this step bunching, we develop a microscopic theory that describes step dynamics during annealing. Based on this theory, we propose a formation mechanism that attributes the cause of step bunching to AsH<sub>x</sub> attached to step edges. We assume that AsH<sub>x</sub> attached to step edges induces irreversible detachment and incorporation processes for Ga atoms terminating step edges, generating a net upward mass transfer across step edges. This results in the formation of step bunches. By assuming a reasonable coverage of AsH<sub>x</sub> at step edges the complicated dependence of the size of the stationary step bunches on annealing conditions can be explained. [S0163-1829(98)08408-2]

### I. INTRODUCTION

A regular monostep array can become unstable and break up into regions with high step density and regions with little or no steps; this is the phenomenon called step bunching. Recent studies show that step bunching is a very common phenomenon observed on many surfaces.<sup>1</sup> Vicinal GaAs(001) is not an exception, and step bunches were observed on layers grown by metal-organic chemical-vapor deposition (MOCVD).<sup>2-6</sup> The characteristics and dynamics of this step bunching have been studied extensively,<sup>4-6</sup> motivated by the expectation that step bunches may serve as templates for fabricating nanostructures.<sup>7</sup> In spite of these studies, a general consensus concerning this step bunching has not been reached. Even the formation mechanism remains an open question.<sup>4-6</sup> This is because epitaxial growth, in which many factors influence the dynamics, is very complicated.

In a previous paper,<sup>8</sup> we showed that step bunches similar to those observed on layers grown by MOCVD form upon annealing vicinal GaAs(001) in AsH<sub>3</sub>/H<sub>2</sub> ambient. The characteristics, surface morphology, and dynamics of these two types of step bunches are very similar; thus we conclude that they are due to the same cause. Foregoing studies revealed that the growth of this step bunch stops after it reaches a particular size.<sup>9</sup> The surface reaches a *stationary state* in AsH<sub>3</sub>/H<sub>2</sub> ambient. Step bunch in its stationary stage is most suited to characterizing its dynamics.

In this paper, we report on how stationary step bunches depend on the annealing conditions such as the partial pressure of AsH<sub>3</sub> (PAsH<sub>3</sub>), annealing temperature, and miscut

direction of the substrate. The annealing conditions studied cover most of the conventional ambients in which MOCVD epitaxial growth is executed. Under all of the experimental conditions, and on all of the substrates studied, we always observed step bunching, not a regular monostep array. Therefore, we conclude that the surface of vicinal GaAs(001) annealed in AsH<sub>3</sub>/H<sub>2</sub> ambient has a general tendency to exhibit step bunches.

Based on that finding, we conclude that AsH<sub>3</sub>/H<sub>2</sub> is the direct cause of step bunching. In order to understand the experimental results, we propose a microscopic theory (DDI model: detachment, diffusion, and incorporation) which describes step dynamics during annealing. Based on the DDI model, a formation mechanism of step bunching is proposed, which assumes a net upward mass transfer across step edges induced by AsH<sub>x</sub> attached to step edges. This model enables us to understand the complicated dependence of the step bunch sizes on annealing conditions, by assuming a reasonable coverage of AsH<sub>x</sub> at step edges.

### II. EXPERIMENT

We used three types of vicinal substrates miscut toward [100], [110]A (A substrates), and [1 $\bar{1}$ 0]B (B substrates), with the miscut angle of 2.0° fixed in this study. Studies concerning other miscut angles can be found in other work.<sup>5,6</sup> Substrates were Si-doped with a carrier concentration of  $4 \times 10^{17}$  cm<sup>-3</sup>. Dopants are shown to have no influence on the formation of step bunches.<sup>10</sup> The annealing process is very similar to that of MOCVD growth; the only difference is that no III species is exposed; thus there is no crystal growth. Before annealing, the sample was cleaned by

$\text{H}_2\text{SO}_4$ , followed by chemical etching in an  $\text{H}_2\text{SO}_4:\text{H}_2\text{O}_2:\text{H}_2\text{O}=4:1:1$ , solution. Next, the substrate was placed on a GaAs-coated carbon susceptor and annealed to the growth temperature by radiation field heating. The total pressure during annealing was  $1.3 \times 10^4$  Pa, and the typical flow rate of  $\text{H}_2$  was 4000 SCCM (SCCM denotes cubic centimeter per minute at STP). The rates of increase and decrease of temperature were  $50^\circ\text{C}$  and  $100^\circ\text{C}$  per minute. During cooling, the sample was exposed to  $\text{AsH}_3/\text{H}_2$ .

The tunneling current and voltage were in the range of  $0.9\text{--}3$  nA and  $-1.8$  to  $-3.0$  V, respectively. Similar scanning tunneling microscopy (STM) images were obtained with the tunneling voltage and current in this range. The resolution of our STM observations is sufficient to resolve a single step if it is located on a very wide terrace, but not if it is in the bunched regions. On GaAs(100) surfaces, a single step is observed by atomic force microscopy (AFM) in air ambient. These results imply that a single-step corrugation remains, even on an oxidized surface, which is observable by STM and AFM. Deterioration of the resolution of STM due to contamination is common when observing atoms in ultra-high vacuum, though when observing large-scale objects, such as these step bunches, it does not seriously influence the images.

### III. RESULTS—STEP BUNCHES IN ITS STATIONARY STATE

To confirm that we are not observing an intermediate stage, the time evolution of step bunches was investigated to determine the annealing time necessary to reach a stationary stage. Figure 1 shows the time evolution of the mean size of step bunches of GaAs(001)-[100] $2^\circ$  annealed at 600 and  $700^\circ\text{C}$  with  $\text{PAsH}_3=1$  Torr. What we refer to as the size of a step bunch is shown in the inset of Fig. 1. Figure 1 shows that the growth of step bunches stops at a certain size.<sup>9</sup> Based on this time evolution, we determined that step bunches evolve to a stationary stage with an annealing time of 5 s at  $700^\circ\text{C}$  and 40 min at  $600^\circ\text{C}$ , respectively. To ensure that the surface has reached the stationary stage, we prepared two substrates, annealed for 5 s and 20 min at  $700^\circ\text{C}$ , and for 40 and 60 min at  $600^\circ\text{C}$  for every set of experimental conditions, and compared their surface morphologies, to check that there was no major difference between them. This confirmed that the surface had reached a stationary state.

Figures 2 and 3 show STM images of stationary step bunches on substrates miscut toward  $[110]_A$ , and  $[1\bar{1}0]_B$ , with  $\text{PAsH}_3$  of  $1 \times 10^{-2}$  low pressure (LP),  $1 \times 10^{-1}$  medium pressure (MP), and 1 Torr high pressure (HP) annealed at  $700^\circ\text{C}$  high temperature (HT) and  $600^\circ\text{C}$  low temperature (LT), respectively. Periodical strips, observed on the image, running against the miscut direction represent facets composed of several monosteps.<sup>8</sup> No or few steps exist between these facets and this region is assumed to be a (100) terrace. Step bunching is observed. These STM images clearly demonstrate that the surface morphology of stationary step bunches depends on annealing conditions. Various step bunches differing in size and shape are observed. We analyze this dependence from three standpoints; (1) existence of branches, (2) degree of fluctuation of step edges, and (3) the variation of the step bunches size.

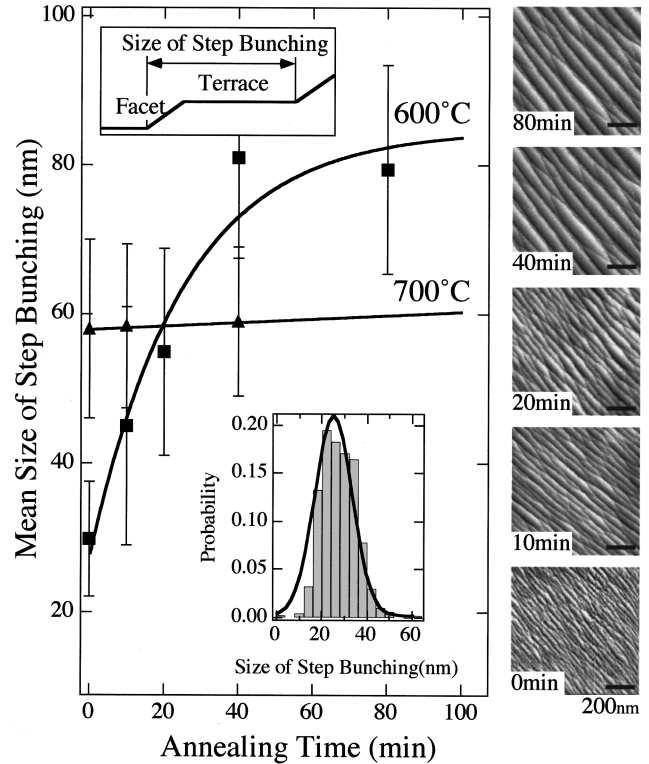


FIG. 1. The mean size of step bunches vs annealing time (squares  $600^\circ\text{C}$ ; triangles,  $700^\circ\text{C}$ ).  $\text{PAsH}_3=1$  Torr. The mean size of step bunches was deduced from a Gaussian curve fitted to the histogram of step bunches sizes, as shown in the inset. The solid line is drawn as a guide for the eye. STM images on the right show the evolution of step bunches on GaAs(001)-[100] $2^\circ$  at  $600^\circ\text{C}$  with the annealing time shown on the images. Scale is  $1000 \times 1000$  nm $^2$ .

(1) Besides the facets, STM images in Figs. 2 and 3 show branches connecting two facets, making the surface resemble a mesh. These branches are not single monosteps but are composed of several monosteps.<sup>9</sup> These branches were observed on all of the substrates under most of the annealing conditions in this study and are thought to comprise a basic component of this step bunching. More detailed discussions regarding the appearance and alignment of these branches are presented elsewhere.<sup>1</sup>

(2) Step edges of the facets of step bunches are not completely straight. The degree of fluctuation depends on the annealing conditions. The straightest step edges were observed on  $B$  substrates annealed in the HT-HP region ( $\text{PAsH}_3 \approx 1$  Torr,  $700^\circ\text{C}$ ). Similar annealing conditions are actually used to fabricate fractional layer superlattices.<sup>12</sup> In the HT-HP region, step edges on the  $B$  substrates ( $B$  steps) are straighter than those on the  $A$  substrates ( $A$  steps), while in the HT-MP region ( $\text{PAsH}_3 \approx 1$  Torr,  $700^\circ\text{C}$ ) there is no conspicuous differences, and in the HT-LP region ( $\text{PAsH}_3 \approx 1 \times 10^{-2}$  Torr,  $700^\circ\text{C}$ )  $A$  steps become straighter. Generally, it is believed that  $B$  steps are straighter in MOCVD ambient;<sup>2</sup> however, our STM images show that  $A$  steps become straighter than  $B$  steps in the HT-LP region. On the other hand, at  $600^\circ\text{C}$ ,  $B$  steps are slightly straighter than  $A$  steps.

This can be explained by combining experimental results of reflectance difference spectroscopy<sup>13</sup> (RDS) and STM.<sup>2,14</sup>

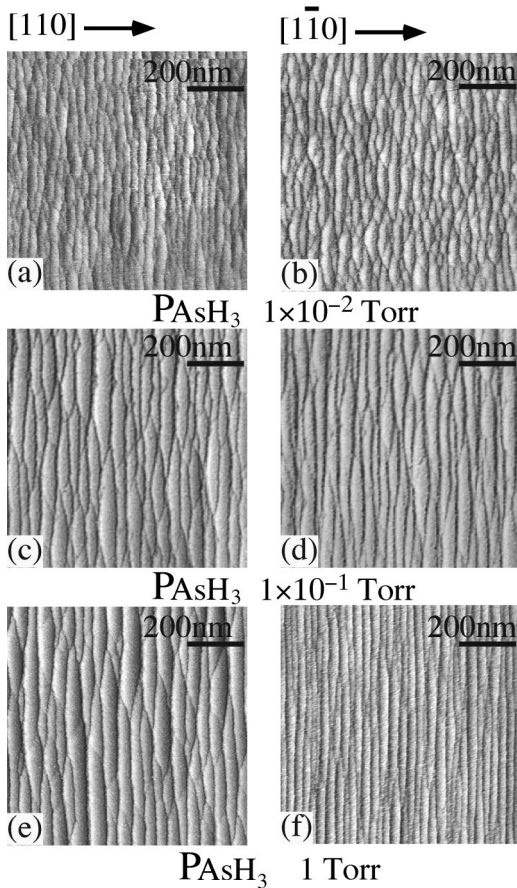


FIG. 2. STM images showing the surface morphology of stationary step bunches on vicinal GaAs(001) annealed at 700 °C. The left and right rows show the surfaces of GaAs(001)-[110] $2^\circ$  and  $-\overline{[110]}2^\circ$ , respectively. (a), (b)  $\text{PAsH}_3=1\times 10^{-2}$  Torr, (c), (d)  $\text{PAsH}_3=1\times 10^{-1}$  Torr and (e), (f)  $\text{PAsH}_3=1$  Torr. Scale is  $900\times 890$  nm $^2$ .

The phase diagram of GaAs as a function of  $\text{PAsH}_3$  and annealing temperature measured by RDS is displayed in Fig. 4 along with our annealing conditions, which are marked by crosses. At 700 °C the surface reconstruction is a mixed structure of  $c(4\times 4)/d(4\times 4)$  and  $(2\times 4)$  in the HP region. As  $\text{PAsH}_3$  is decreased, it switches to  $(2\times 4)$ . STM observations indicate that the two reconstructions have different types of straight step edges; the  $(2\times 4)$  reconstruction has straight  $A$  and rough  $B$  step edges $^{14}$  while the opposite holds true for the  $c(4\times 4)$  reconstruction. $^2$  Thus, the observed reversal of straight step edges is indirect evidence that the surface reconstruction is  $c(4\times 4)$  in the HT-HP region and switches to  $(2\times 4)$  in the HT-LP region. The reason why these reconstructions have different straight steps is unknown. $^{15}$

(3) The size of stationary step bunches depends on the annealing condition in a complicated fashion. This is illustrated in Fig. 5, which shows the size of stationary step bunches on  $A$  and  $B$  substrates versus  $\text{PAsH}_3$  at 600 and 700 °C. Several important points are observed in Fig. 5. First, it is easy to see that when all of the annealing conditions are the same, except the annealing temperature, the size of step bunches on a substrate annealed at 600 °C is always larger than that annealed at 700 °C. Second, the size of step

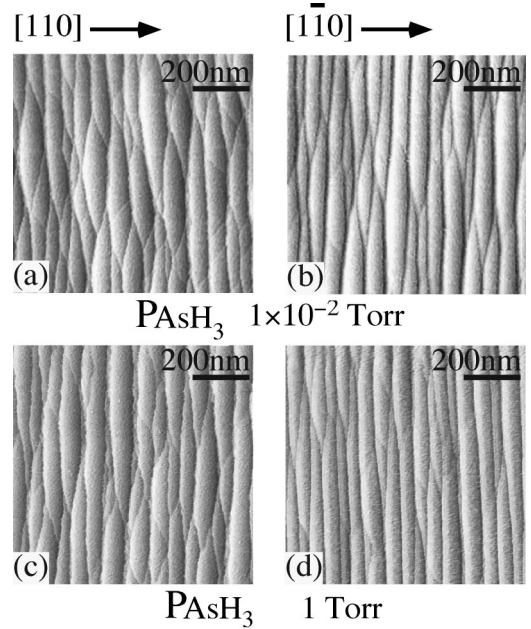


FIG. 3. STM images showing the surface morphology of stationary step bunches on vicinal GaAs(001) annealed at 600 °C. The left and right rows show the surfaces of GaAs(001)-[110] $2^\circ$  and  $-\overline{[110]}2^\circ$ , respectively. (a), (b)  $\text{PAsH}_3=1\times 10^{-2}$  Torr, (c), (d)  $\text{PAsH}_3=1$  Torr scale is  $900\times 890$  nm $^2$ .

bunches on the  $A$  substrates annealed at 700 °C increases with  $\text{PAsH}_3$ , while that on  $B$  substrates increases once in the MP region and then decreases in the HP region. On the other hand, at 600 °C, the size of step bunches negligibly depends on  $\text{PAsH}_3$  for both the  $A$  and  $B$  substrates. Also, step bunches on the  $A$  substrates is always larger than that on the  $B$  substrates at 600 °C.

#### IV. DISCUSSION—CAUSE OF STEP BUNCHING

##### A. Basics of the DDI process

Since step bunches always form when vicinal GaAs(001) substrates are annealed in  $\text{AsH}_3/\text{H}_2$  ambient for a very wide

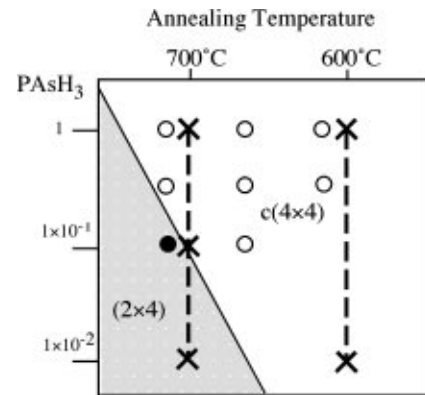


FIG. 4. Phase diagram of GaAs(001) vs temperature and  $\text{PAsH}_3$  measured by reflectance difference spectroscopy (Ref. 13). White and black circles represent the  $c(4\times 4)$  and  $(2\times 4)$  phases, respectively. The crosses indicate the annealing conditions of the surfaces shown in Fig. 2 (left three crosses) and Fig. 3 (right two crosses). Note the phase transition of  $c(4\times 4)\Leftrightarrow(2\times 4)$  occurs in the HT-MP region (700 °C,  $\text{PAsH}_3=0.1$  Torr).

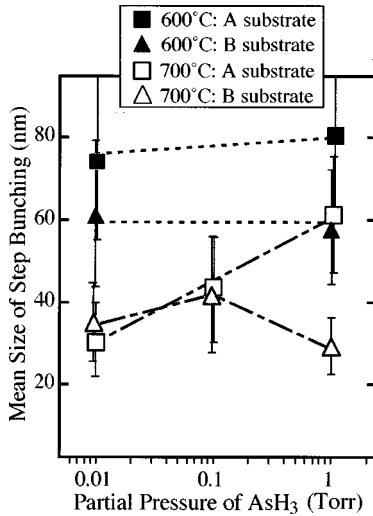


FIG. 5. Mean size of stationary step bunches vs PAsH<sub>3</sub>, annealing temperature (black, 600 °C; white, 700 °C) and miscut direction of substrates (squares; A substrates; triangles, B substrates).

range of experimental conditions, we conclude that AsH<sub>3</sub>/H<sub>2</sub> is the direct cause. Based on this conclusion, we propose a formation mechanism of step bunching to explain the experimental results.

Basically, our model treats the surface of the binary compound GaAs as a quasingle element system. Only migration of Ga atoms on the surface is considered. This is because As atoms released to the surface from step edges (or terraces) will desorb easily to the ambient. AsH<sub>3</sub> will act as a source for As, and once Ga is released to the surface, it is stabilized at some place by As coming from the AsH<sub>3</sub> ambient. The effect of As is embodied in our model via spontaneous desorption of unessential As to the ambient and adsorption of As to stabilize the diffusing Ga. Desorption of Ga atoms is considered to be negligible because it has been reported that nominal desorption occurs even under annealing conditions at which desorption is far more likely to occur than in our experiments.<sup>3</sup>

During annealing, steps can move (thus step bunches develop), only by exchanging step edge Ga atoms with other steps. This exchange proceeds by a successive combination of three fundamental stages (DDI process). First, a step edge Ga atom detaches to the upper or lower boundary terrace (detachment process). Simultaneously, the released As will desorb to the ambient. Next, this Ga atom diffuses across the terraces (diffusion process). Finally, it is incorporated into a step and is stabilized by As coming from the ambient (incorporation process). The abbreviation of DDI is taken from the first letters of the three processes. These processes are characterized by the energy potential barrier around the step edge shown in Fig. 6. Schwoebel's effect<sup>16</sup> is included. We assume nearest-neighbor step-step interaction, which means that diffusion across steps is inhibited. Also, noninteracting diffusing atoms are assumed, which means that we neglect the formation of islands on the terraces by coalescence of diffusing atoms. These approximations are the same as the usual assumptions employed in the Burton, Cabrera, and Frank-type theory,<sup>17</sup> and are well suited to describing the characteristics of annealing processes. Since no desorption or deposition occurs on the surface, the residence time of dif-

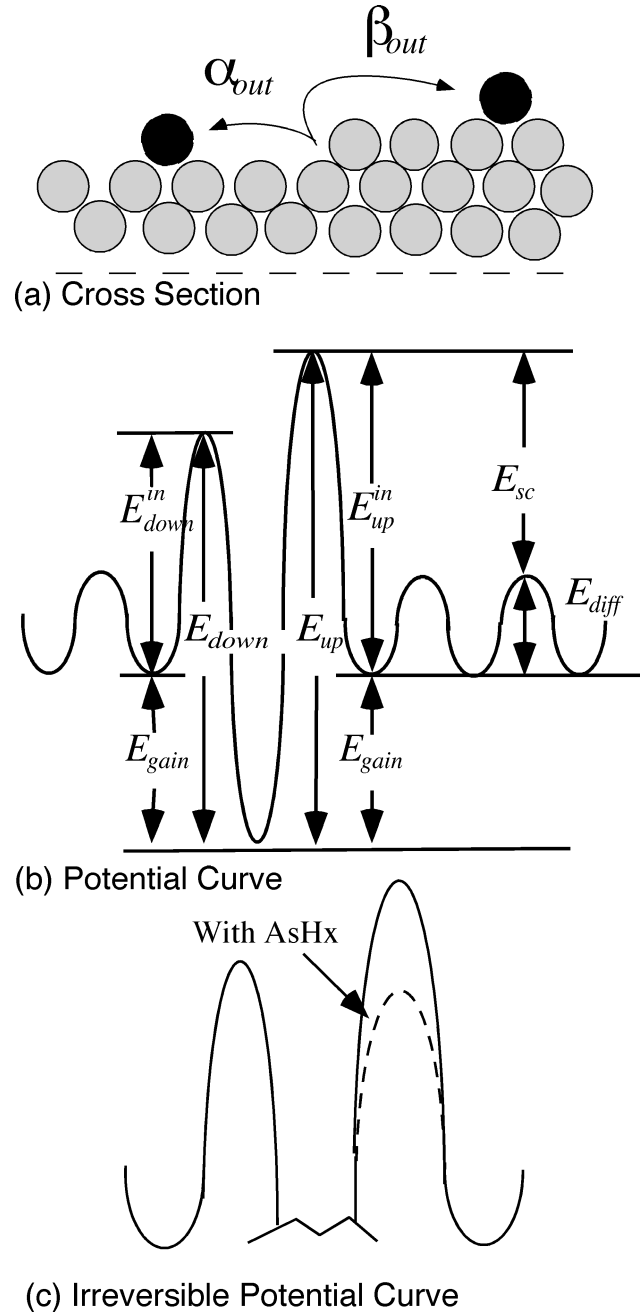


FIG. 6. Step edge potential curve. (a) A crystallographic schematic of a step.  $\alpha_{out}$  and  $\beta_{out}$  are the probabilities of the Ga atom terminating the step edge to detach to the lower and upper bounding terraces, respectively. (b) The potential energy curve around step edges.  $E_{sc}$  is Schwoebel's barrier,  $E_{diff}$  is the activation energy of Ga surface diffusion. (c) The potential-energy curve showing the irreversible detachment and incorporation processes for Ga atoms terminating step edges.

fusing atoms becomes quite long; thus we assume infinitely fast diffusion. The appropriateness of this assumption is supported by the fact that step kinetics is very slow compared to diffusion kinetics.

For simplicity, we consider a one-dimensional monostep train which mimics perfectly straight steps where the location of the  $n$ th step is defined as  $x_n$  and the width of the  $n$ th terrace is  $S_n = x_n - x_{n-1}$  as shown in Fig. 7. The actual degree of fluctuation of step edges is determined by a competition between the formation energy of kinks and the thermal

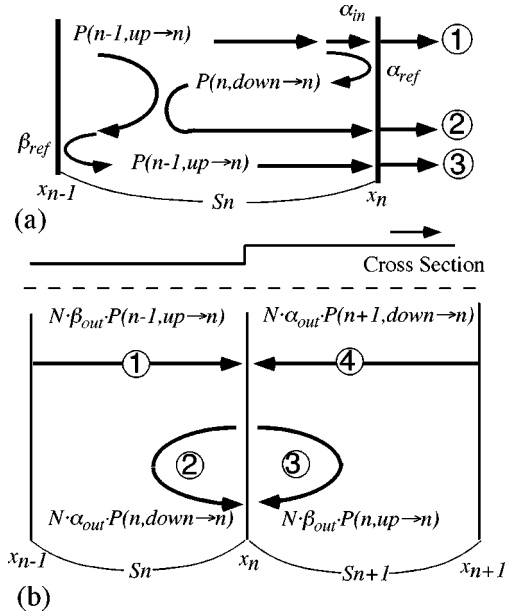


FIG. 7. (a) The three pathways that contribute to  $P(n-1, \text{up} \rightarrow n)$ . The first pathway represents the probability of diffusion across the  $n$ th terrace and direct incorporation into the  $n$ th step. (b) Four possible pathways for an atom to finally be incorporated into the  $n$ th step. The figures show the actual number of atoms included in each pathway per unit time.

fluctuation (entropy of the steps), which is not included in the present form of the DDI model. A series of probability functions ( $P$  series) is defined in which  $P(m, \text{up/down} \rightarrow n)$  expresses the probability of an atom, initially located at the upper/lower site in the immediate vicinity of the  $m$ th step, to diffuse across the surface and finally be incorporated into the  $n$ th step. As shown in Fig. 7(a), assuming the nearest-neighbor interaction, there exists three pathways which contribute to  $P(n-1, \text{up/down} \rightarrow n)$ ;

$$P(n-1, \text{up} \rightarrow n) = P_{\text{go}}(S_n) \alpha_{\text{in}} + P_{\text{go}}(S_n) \alpha_{\text{ref}} P(n, \text{down} \rightarrow n) + P_{\text{back}}(S_n) \beta_{\text{ref}} P(n-1, \text{up} \rightarrow n), \quad (1)$$

where  $P_{\text{go}}(S_n)$  is the probability of an atom initially placed at the edge of a terrace of width  $S_n$  to diffuse across the

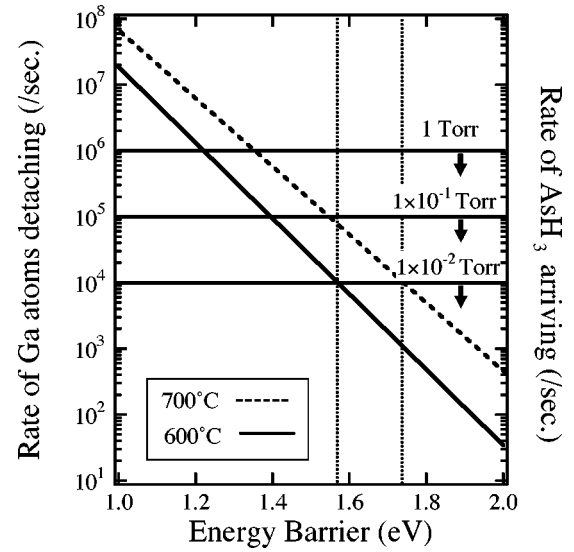


FIG. 8. The rate of Ga atom detachment from step edges ( $\Gamma_{\text{Ga}}$ ) as a function of the activation energy ( $E_{\text{detact}}$ ) at 600 °C (solid line) and 700 °C (dashed line), combined with the calculated rate of  $\text{AsH}_3$  arrival at step edges ( $\Gamma_{\text{AsH}_3}$ ) at each  $\text{PAsH}_3$ . The effective rate of  $\text{AsH}_3$  arrival at step edges will decrease at 700 °C, as indicated by the arrows.

terrace and reach the opposite edge before it diffuses back to its origin, while  $P_{\text{back}}(S_n)$  is the probability of an atom to diffuse back to the origin before reaching the opposite edge of the terrace,  $\alpha$  and  $\beta$  represent probabilities of the occurrence of processes which take place at the lower and upper boundary terraces, subscripts out, in, and ref represent the detachment of Ga atoms from a step edge, the incorporation of a Ga atom into a step edge, and a reflection of a diffusing Ga atom approaching a step edge (e.g.,  $\alpha_{\text{out}}$  is the probability of the step edge Ga atom to detach and move to the lower bounding terrace). By definition,  $\alpha_{\text{out}} + \beta_{\text{out}} = 1$ ,  $\alpha_{\text{in}} + \alpha_{\text{ref}} = 1$ , and  $\beta_{\text{in}} + \beta_{\text{ref}} = 1$ . We assume that the diffusing Ga atoms can be regarded as random walkers. In that case,  $P_{\text{go}}(S_n) = 1/S_n$ , and  $P_{\text{back}}(S_n) = 1 - 1/S_n$ .

A similar equation can be derived for  $P(n, \text{up} \rightarrow n)$ , and these two sets of equations can be solved reflexively, giving the concrete value of the  $P$  series as

$$P(n-1, \text{up} \rightarrow n) = \frac{P_{\text{back}}(S_n) \beta_{\text{in}} + [P_{\text{go}}(S_n) - P_{\text{back}}(S_n)] \beta_{\text{in}} \alpha_{\text{ref}}}{1 - P_{\text{back}}(S_n) (\alpha_{\text{ref}} + \beta_{\text{ref}}) + [P_{\text{back}}(S_n) - P_{\text{go}}(S_n)] \alpha_{\text{ref}} \beta_{\text{ref}}}. \quad (2)$$

The velocity of steps is determined from the difference between the rate of atoms detaching from and incorporating into the step edge which is expressed as

$$\frac{1}{a} \frac{dx_n}{dt} = N - N [\beta_{\text{out}} P(n-1, \text{up} \rightarrow n) + \alpha_{\text{out}} P(n, \text{down} \rightarrow n) + \beta_{\text{out}} P(n, \text{up} \rightarrow n) + \alpha_{\text{out}} P(n+1, \text{down} \rightarrow n)], \quad (3)$$

where  $N$  is the total number of Ga atoms detaching from a step edge per unit time. The origin of each term in Eq. (3) is shown in Fig. 7(b). Consider a system in which all of the terraces have the same width  $d$  except for the  $n$ th terrace with width  $d + \Delta d$ . In this case, the time evolution equation of the  $n$ th terrace becomes

$$\frac{1}{a} \frac{dS_n}{dt} = (\alpha_{\text{out}} \beta_{\text{in}} - \beta_{\text{out}} \alpha_{\text{in}}) \left[ \frac{1}{\alpha_{\text{in}} \beta_{\text{in}} (d + \Delta d) + \alpha_{\text{in}} + \beta_{\text{in}} - 2\alpha_{\text{in}} \beta_{\text{in}}} - \frac{1}{\alpha_{\text{in}} \beta_{\text{in}} d + \alpha_{\text{in}} + \beta_{\text{in}} - 2\alpha_{\text{in}} \beta_{\text{in}}} \right]. \quad (4)$$

This time evolution equation shows that step bunching occurs when

$$\alpha_{\text{out}}\beta_{\text{in}} - \beta_{\text{out}}\alpha_{\text{in}} < 0 \quad (\text{DDI factor}), \quad (5)$$

because  $\alpha_{\text{in}}\beta_{\text{in}} > 0$  and  $\alpha_{\text{in}} + \beta_{\text{in}} - 2\alpha_{\text{in}}\beta_{\text{in}} > 0$ . Equation (5) is similar to the results obtained by Schwoebel's and Shipsey.<sup>16</sup> (They considered the case of crystal growth, giving  $\beta_{\text{in}} > \alpha_{\text{in}}$  as a criterion for step bunching to occur which corresponds to the case of  $\alpha_{\text{out}} = 1$  and  $\beta_{\text{out}} = 1$ .) Equation (5) shows that step bunching occurs when an upward net mass transfer across step edges exists because  $\alpha_{\text{out}}\beta_{\text{in}}$  and  $\beta_{\text{out}}\alpha_{\text{in}}$  represent the downward and upward mass transfers across step edges, respectively. Step bunching occurs even on an initially perfect monostep train because the thermal fluctuation, however small it is, will be constantly enhanced, as Eq. (5) shows, and finally result in step bunching.

The four probabilities in Eq. (4) are characterized by the ideal energy potential around the step edge shown in Fig. 8, as

$$\alpha_{\text{out}} = \frac{\exp(-E_{\text{down}}/kT)}{\exp(-E_{\text{down}}/kT) + \exp(-E_{\text{up}}/kT)}, \quad (6)$$

$$\beta_{\text{out}} = \frac{\exp(-E_{\text{up}}/kT)}{\exp(-E_{\text{down}}/kT) + \exp(-E_{\text{up}}/kT)}, \quad (7)$$

$$\begin{aligned} \alpha_{\text{in}} &= \frac{\exp(-E_{\text{down}}^{\text{in}}/kT)}{\exp(-E_{\text{down}}^{\text{in}}/kT) + \exp(-E_{\text{diff}}/kT)} \\ &\approx \exp\{-(E_{\text{down}}^{\text{in}} - E_{\text{diff}})/kT\}, \end{aligned} \quad (8)$$

$$\begin{aligned} \beta_{\text{in}} &= \frac{\exp(-E_{\text{up}}^{\text{in}}/kT)}{\exp(-E_{\text{up}}^{\text{in}}/kT) + \exp(-E_{\text{diff}}/kT)} \\ &\approx \exp\{-(E_{\text{up}}^{\text{in}} - E_{\text{diff}})/kT\}, \end{aligned} \quad (9)$$

where  $E_{\text{down}}^{\text{in}}$ ,  $E_{\text{up}}^{\text{in}}$ ,  $E_{\text{gain}}$ ,  $E_{\text{down}}$ , and  $E_{\text{up}}$  are the energy heights shown in Fig. 8, and  $k$  and  $T$  have their usual meanings. Another important property of the DDI factor is that  $\alpha_{\text{out}}\beta_{\text{in}}$  and  $\beta_{\text{out}}\alpha_{\text{in}}$  have a general tendency to cancel out, thus the DDI factor is usually very small, in fact, close to zero. This can be understood by considering

$$\begin{aligned} \frac{\alpha_{\text{in}}}{\beta_{\text{in}}} &= \frac{\exp\{-(E_{\text{down}}^{\text{in}} - E_{\text{diff}}/kT)\}}{\exp\{-(E_{\text{up}}^{\text{in}} - E_{\text{diff}}/kT)\}} \\ &= \frac{\exp\{-(E_{\text{down}}^{\text{in}} + E_{\text{gain}})kT\}}{\exp\{-(E_{\text{up}}^{\text{in}} + E_{\text{gain}})kT\}} \\ &= \frac{\exp(-E_{\text{down}}/kT)}{\exp(-E_{\text{up}}/kT)} = \frac{\alpha_{\text{out}}}{\beta_{\text{out}}}. \end{aligned} \quad (10)$$

Equation (10) represents nothing other than the general understanding that kinetic effects do not influence the surface morphology in equilibrium. This is true for the surface of clean vicinal GaAs(001), and STM studies suggest that only weak or no interaction exists among steps on this surface.<sup>18</sup>

## B. The DDI model

The DDI factor can take nonzero values in particular situations. We propose that Ga atoms follow an energy potential curve different at step edges from the usual one when  $\text{AsH}_x$  is attached to the Ga atoms.  $\text{AsH}_x$  represents by-products produced by dissociation of  $\text{AsH}_3$  at step edges. A Ga atom detaches from or is incorporated into step edges according to the dashed potential line when  $\text{AsH}_x$  is attached to it, and otherwise follows the usual potential curve indicated by the solid line, as shown in the schematic in Fig. 6(c). Strictly speaking,  $\text{AsH}_x$  influences both the upper and lower energy potentials at step edges; however, for simplicity, we assume that  $\text{AsH}_x$  influences only the upper energy potential in our model. We make the assumption that the activation energy required for Ga atoms to detach from (to be incorporated into) the upper terrace with  $\text{AsH}_x$  is lower than the usual case with no  $\text{AsH}_x$ . In this case, the averaged DDI factor becomes negative, and an upward net movement of atoms across step edges emerges, which leads to step bunching. This is because Ga atoms terminating step edges reside there for a long time, compared to the time the diffusing Ga atoms stay at step edges before incorporation, and thus have a greater possibility of  $\text{AsH}_x$  attaching to them. This effect is incorporated into the DDI factor as a larger amount of increase of  $\beta_{\text{out}}$  (due to the decrease in the energy barrier height) compared to  $\beta_{\text{in}}$  resulting in a negative DDI factor. This proposal is analogous to introducing irreversible detachment and incorporation processes at step edges. We use the term stationary instead of equilibrium because of this irreversible process; the surface is not actually in its real equilibrium because of the presence of  $\text{AsH}_3/\text{H}_2$  ambient, and kinetic effects induced by this ambient can influence the surface morphology. Our model can account for the observed bunching when the substrate is annealed in  $\text{AsH}_3/\text{H}_2$  ambient and the debunching (not shown) when a bunched substrate is annealed in ambient other than  $\text{AsH}_3/\text{H}_2$ .

The driving force of step bunching (DDI force),  $F_{\text{SB}}$ , is proportional to

$$\begin{aligned} F_{\text{SB}} \propto & \theta_{\text{AsH}_x} (\alpha_{\text{out}}^{\text{AsH}_x} \beta_{\text{in}}^{\text{AsH}_x} - \beta_{\text{out}}^{\text{AsH}_x} \alpha_{\text{in}}^{\text{AsH}_x}) + (1 - \theta_{\text{AsH}_x}) \\ & \times (\alpha_{\text{out}}^{\text{clean}} \beta_{\text{in}}^{\text{clean}} - \beta_{\text{out}}^{\text{clean}} \alpha_{\text{in}}^{\text{clean}}), \end{aligned} \quad (11)$$

where  $\theta_{\text{AsH}_x}$  is the coverage of  $\text{AsH}_x$  attached to Ga atoms at the step edges, and superscripts  $\text{AsH}_x$  and ‘‘clean’’ represent with and without  $\text{AsH}_x$ . As mentioned above, the second term in Eq. (11) is close to zero, thus  $F_{\text{SB}}$  is proportional to  $\theta_{\text{AsH}_x}$ .

If the DDI force is the only interaction among steps, then step bunches will grow to infinite size. This is because the DDI force acts as an attractive interaction among steps (in our model) and there is no repulsive interaction that counterbalances it. However, this is clearly inconsistent with the results of experiments. It is now well established that elastic<sup>19</sup> and entropic-repulsive interactions<sup>20</sup> exist among steps. Both these repulsive forces decrease according to the power law of  $\sim 1/d^2$ , where  $d$  is the distance between steps, while the DDI force decreases with the power law of  $\sim 1/d$ .<sup>21</sup> Thus, the repulsive forces are short ranged com-

pared to the DDI force. Computer simulations and numerical analysis in which the DDI effect is combined with the repulsive interactions, show that the width of the terrace ( $\sim 50$  nm) is primarily determined by the DDI force, the step-step distance ( $\sim 2$  nm) in the facet by the repulsive interactions, and that the size of stationary step bunches increases with the DDI force.<sup>21</sup>

The DDI model indicates that the size of stationary step bunches increases with the DDI force, and thus with  $\theta_{\text{AsH}_x}$ .

### C. Explanation of the experimental results using the DDI model

We show that the dependence of the size of stationary step bunches can be understood by assuming a reasonable  $\theta_{\text{AsH}_x}$ . An important factor that must be considered is the atomic structure of steps. Usually, it is assumed that *A* steps are Ga-terminated while *B* steps are As-terminated. Since the main process that contributes to the formation of step bunches in the DDI model is the detachment of Ga atoms from step edges, the DDI model is best suited to describing the characteristics of step bunches on *A* substrates.

At a low annealing temperature, 600 °C, the rate of Ga atoms detaching from step edges is low and the residence time of  $\text{AsH}_x$  at step edges is long, a situation likely to result in high  $\theta_{\text{AsH}_x}$ . We assume that  $\theta_{\text{AsH}_x} \approx 1$  at 600 °C regardless of  $\text{PAsH}_3$ . This explains why the size of stationary step bunches does not depend on  $\text{PAsH}_3$  at 600 °C for both *A* and *B* substrates. In contrast, at a higher annealing temperature of 700 °C, we assume that  $\theta_{\text{AsH}_x} < 1$  within the  $\text{PAsH}_3$  range employed in our experiments. This explains why step bunches on substrates annealed at 600 °C are always larger than those annealed at 700 °C. Since  $\theta_{\text{AsH}_x}$  at *A* steps increases with  $\text{PAsH}_3$ , the size of stationary step bunches increases with  $\text{PAsH}_3$  for *A* substrates at 700 °C.

On the other hand, the situation is more complicated at *B* steps since they are terminated with As. It is possible that similar irreversible detachment and incorporation processes induced by  $\text{AsH}_x$  occur at *B* steps. However if this is so, it must be a complicated process, e.g., the terminating As atom must detach from step edges simultaneously with or before the Ga atom detaches to the terrace. Also, this Ga atom is bound rigidly to the substrate via four Ga-As chemical bonds (in the case of an ideal step edge). Therefore, we assume that kinks in *B* steps, which are fragments of *A* steps (*A*-type kinks), provide sites at which the irreversible detachment and incorporation process occurs. *B* steps have a low density of *A*-type kinks, which would give a smaller net DDI force, and thus smaller stationary step bunches. This explains why step bunches on *B* substrates at 600 °C are smaller than those on *A* substrates, when  $\theta_{\text{AsH}_x} \approx 1$  for both substrates in the DDI model. It is also possible to understand the slight decrease of the size of step bunches on *B* substrates in the HT-HP region for a similar reason. STM images of *B* substrates annealed in the HT-HP region show very straight step edges and few branches, which means a low density of *A*-type kinks. We suppose that this decrease in density overwhelms the increase of  $\theta_{\text{AsH}_x}$  due to the high  $\text{PAsH}_3$ , thus leading to small step bunches in the HT-HP region.

### D. Quantitative analysis

A simple quantitative analysis is provided to show that assumptions regarding  $\theta_{\text{AsH}_x}$  are reasonable. We calculate the rate of  $\text{AsH}_3$  arriving at step edges ( $\Gamma_{\text{AsH}_3}$ ) and the rate of Ga atoms detaching from step edges ( $\Gamma_{\text{Ga}}$ ) to the bounding terraces as a function of the activation energy of detachment ( $E_{\text{detach}}$ ). We assume that  $\theta_{\text{AsH}_x}$  is determined mainly by a competition between these two factors. When  $\Gamma_{\text{AsH}_3} > \Gamma_{\text{Ga}}$ , we assume  $\theta_{\text{AsH}_x} \approx 1$ , and in the opposite case  $\theta_{\text{AsH}_x} < 1$ . Assumptions concerning  $\theta_{\text{AsH}_x}$  limit  $E_{\text{detach}}$  into a particular range. Subsequently, we show that the estimated activation energy is reasonable, by comparing it with values estimated by other researchers. This supports the appropriateness of the DDI model.

Simple thermodynamic calculations give  $\Gamma_{\text{AsH}_3} = \frac{1}{4} n \bar{v}$ , where  $n$  is the density and  $\bar{v}$  is the mean velocity of  $\text{AsH}_3$ . The vibration frequency of Ga atoms is assumed to be  $\sim 10^{13}$ /s. Figure 8 shows the estimated  $\Gamma_{\text{Ga}}$  as a function of  $E_{\text{detach}}$  at 600 and 700 °C, combined with the calculated  $\Gamma_{\text{AsH}_3}$  at each  $\text{PAsH}_3$ . In the DDI model, we assume that  $\theta_{\text{AsH}_3} \approx 1$  at 600 °C, which imposes  $\Gamma_{\text{AsH}_3} > \Gamma_{\text{Ga}}$  at  $\text{PAsH}_3$  yields of  $1 \times 10^{-2}$  Torr. This gives  $E_{\text{detach}} \geq 1.6$  eV. On the other hand, at 700 °C, the DDI model suggests  $\theta_{\text{AsH}_x} < 1$ . Figure 8 shows that  $\Gamma_{\text{Ga}} (E_{\text{detach}} \sim 1.6 \text{ eV}, 700 \text{ °C}) \cong \Gamma_{\text{AsH}_3}$  at  $\text{PAsH}_3 = 1 \times 10^{-1}$  Torr, which means that in our model,  $\theta_{\text{AsH}_x} \sim 1$  above this  $\text{PAsH}_3$ . At first sight, this seems to contradict the DDI model. This incompatibility is due to the rate of  $\text{AsH}_3$  arriving at step edges not being equal to the rate of  $\text{AsH}_x$  attaching to step edges. These two rates are related via the sticking probability of  $\text{AsH}_3$  and the finite residence time of  $\text{AsH}_x$  at step edges, which themselves depend on temperature. When compared to 600, at 700 °C, a smaller sticking probability and a shorter residence time are inferred, which implies a decrease in the rate of  $\text{AsH}_x$  attaching to step edges. In fact, enhanced detachment of  $\text{AsH}_x$  at step edges is observed.<sup>22</sup> This effect is included in Fig. 8 as an apparent decrease in the rate of  $\text{AsH}_3$  arriving at 700 °C, as indicated by the arrows in the figure. We conclude that it is possible to maintain  $\theta_{\text{AsH}_x} < 1$  regardless of  $\text{PAsH}_3$  at 700 °C by taking these factors into account.

The DDI model imposes  $E_{\text{detach}} \geq 1.6$  eV. Unfortunately, to the best of the authors' knowledge, there is no direct information available on this activation energy. The activation energy of detachment is comprised of the activation energy of surface diffusion,  $E_{\text{diff}}$ , which is estimated (on various surfaces) to be around 0.5–1.0 eV,<sup>22–26</sup> Schwoebel's barrier  $E_{sc}$ , 0.2–0.6 eV (Ref. 27), and the energy gain  $E_{\text{gain}}$ , as shown in Fig. 6(b). The only direct measurement of activation energy concerning detachment is of the effective activation energy of step rearrangement on Si(100),  $1.3 \pm 0.3$  eV.<sup>28</sup> Considering these results, we conclude that  $E_{\text{detach}} \geq 1.6$  eV is a reasonable estimation.

The activation energy of surface diffusion on GaAs(001) was determined using reflection high-energy electron-diffraction oscillation as  $E = 1.58 + n \times 0.15$  (eV), where  $n$  is the number of nearest-neighbor sites.<sup>29</sup> This estimation is an effective activation energy that incorporates the average sur-

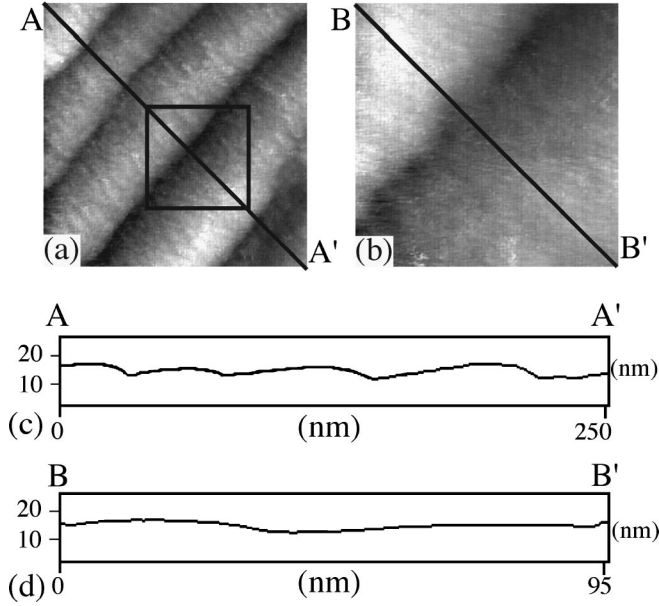


FIG. 9. (a) High-resolution STM images of step bunching on vicinal GaAs(001)-[100] $2^\circ$ . The scale is  $180 \times 180 \text{ nm}^2$ . The ordinate scale is also in nm. (b) Magnified STM image of the box shown in (a). Scale is  $70 \times 70 \text{ nm}^2$ . (c) AA' corresponds to the average cross section on the line shown in (a). (d) BB' to the average cross section on the line shown in (b). The cross sections were taken along the miscut direction.

face diffusion processes as well as the incorporation and detachment processes associated with step edges.<sup>29</sup> Since  $E_{\text{detach}} > E_{\text{diff}}$  this estimation indirectly supports  $E_{\text{detach}} > 1.58 \text{ eV}$ , which is very similar to our result.

### E. Other possible origins

We discuss whether or not other known formation mechanisms of step bunching can explain our experimental results consistently. Possible causes of step bunching are faceting,<sup>30</sup> coexistence of different reconstructions,<sup>20</sup> Frank impurities,<sup>31</sup> electromigration,<sup>32</sup> and pinning.<sup>33</sup> Several of these can be eliminated by *a priori* conditions. We can exclude electromigration since our substrates are annealed by radiation and no direct current was applied. Also, Frank impurities can be safely excluded, because it basically considers crystal growth and the doping level used in this study does not influence the surface morphology. Also dopants are directly shown not to be the cause of this step bunching.<sup>10</sup> Pinning is eliminated because, unlike in our case, step bunches formed by this process are not periodic.<sup>33</sup>

The most well-known cause of step bunching is faceting.<sup>30</sup> Since the free energy of the facet (bunched region) is relatively low, from a microscopic standpoint, generally they form a well-defined plane with a relatively low Miller index.<sup>30</sup> However regarding this step bunching, high-resolution STM images indicate that the facet edges are not sharp and steps in the facet are not regulated periodically, which means that the facets do not form a well-defined plane, as displayed in Fig. 9. The cross sections of the terraces and facets shown in Figs. 9(c) and 9(d) show that the steps are bound loosely in the faceted region, forming a gentle slope rather than a well-defined sharp facet.

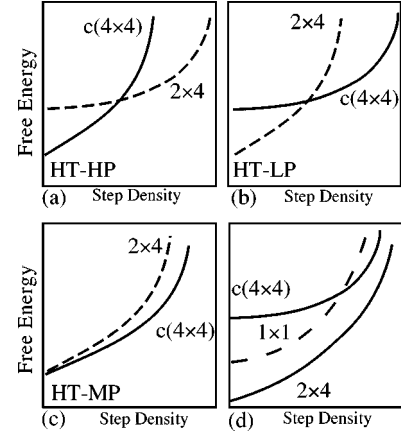


FIG. 10. Free-energy curve in the (a) HT-HP region, and (b) HT-LP region, when step bunching forms. The solid and dashed curves represent the free energy of  $c(4 \times 4)$  and  $2 \times 4$  reconstructions. (c) Free-energy curve at the critical point of  $2 \times 4 \Leftrightarrow c(4 \times 4)$ , which is in the HT-MP region. No step bunching occurs. (d) Overall free-energy curve of three combined phases where the surface reconstruction is  $(2 \times 4)$  with no step bunching.

Also, thermodynamic faceting can occur when two phases coexist on a surface.<sup>20</sup> The surface free-energy curve is expressed as a function of step density ( $\tan \theta$ ) as

$$f_{\text{surface}}^n(\theta, T, P_{\text{AsH}_3}) = f_{\text{terr}}^n(T, P_{\text{AsH}_3}) + \beta^n(T, P_{\text{AsH}_3}) \tan \theta + G^n(T, P_{\text{AsH}_3}) \tan^3 \theta, \quad (12)$$

where the surface reconstruction is represented by the superscript  $n$ , and  $f_{\text{surface}}^n$ ,  $f_{\text{terr}}^n$ ,  $\beta^n$ , and  $G^n$ , are the total free energy, surface tension of the terrace, step formation energy, and the free energy of step-step interaction, respectively.<sup>20</sup> From the phase diagram in Fig. 4, we select  $c(4 \times 4)$  and  $(2 \times 4)$  phases as the two coexisting reconstructions. Indeed, our STM images show that the mean distance among steps in the faceted region is around four times the length of the  $1 \times 1$  unit cell. Details of the shape of the free-energy curve for these reconstructions are not known, though, in the HT-HP region the surface reconstructs to the  $c(4 \times 4)$  phase, thus  $f_{\text{terr}}^{2 \times 4} > f_{\text{terr}}^{c(4 \times 4)}$ . Similarly,  $f_{\text{terr}}^{2 \times 4} < f_{\text{terr}}^{c(4 \times 4)}$  in the HT-LP region.

Step bunches form when the two free-energy curves intersect and form an overall nonconvex curve in the manner displayed in Fig. 10(a) for the HT-HP region and in Fig. 10(b) for the HT-LP region. Regarding the RDS phase diagram shown in Fig. 4, the critical point of the  $c(4 \times 4) \Leftrightarrow (2 \times 4)$  phase transition is near the HT-MP region. This is also supported by the fact that the degrees of fluctuation of step edges of step bunches on the A and B substrates are similar in this region. At the critical point,  $f_{\text{terr}}^{c(4 \times 4)} = f_{\text{terr}}^{(2 \times 4)}$ ; thus it is impossible to form an overall convex curve as shown in Fig. 10(c). Step bunching does not occur at the critical point. However, this prediction completely conflicts with our experimental results.

One way to overcome this incompatibility is to introduce another reconstruction, e.g., the  $1 \times 1$  phase. In this case we must consider a combined free energy of three or more curves. However results of various STM studies<sup>14,18</sup> show

that a regular monostep array forms on the vicinal surface reconstructed to  $(2 \times 4)$ , which means that the free-energy curve of the  $(2 \times 4)$  phase does not intersect with the free-energy curve of other reconstructions (if it does, step bunching should occur). This aspect is shown in Fig. 10(d). Therefore, this mechanism cannot explain why step bunching occurs on substrates annealed in the HT-LP region where the surface reconstruction is  $(2 \times 4)$ .

## V. CONCLUSION

We systematically studied the characteristics of stationary step bunches formed on vicinal GaAs(001) in AsH<sub>3</sub>/H<sub>2</sub> ambient under a wide range of annealing conditions, and found that stationary step bunches strongly depend on the annealing conditions such as annealing temperature, PAsH<sub>3</sub>, and the miscut direction of the substrate. Since step bunching always occurred when vicinal GaAs(001) was annealed in AsH<sub>3</sub>/H<sub>2</sub> ambient, we concluded that AsH<sub>3</sub>/H<sub>2</sub> is the direct cause of step bunching and modeled the formation mechanism based on a microscopic theory that describes step dy-

namics during annealing (the DDI model). The DDI model is particularly appropriate for describing step dynamics under conditions with no desorption or deposition. The time evolution equation of a step array was deduced by estimating the total balance of the number of atoms detaching from and being incorporated into the step edges, which shows that step bunching occurs when the DDI factor is negative, which corresponds to the existence of an upward mass transfer across step edges. Based on this result, we proposed that AsH<sub>x</sub> attached to Ga atoms terminating step edges induces an irreversible detachment and incorporation process for these Ga atoms, resulting in a negative DDI factor. This model can account for the formation of step bunches when the substrate is annealed in AsH<sub>3</sub>/H<sub>2</sub> ambient and for the debunching observed when the bunched substrate is annealed in ambient other than AsH<sub>3</sub>/H<sub>2</sub>. AsH<sub>x</sub> is an indispensable factor for this step bunching to occur. Using this model we can understand the complicated dependence of the size of step bunches on annealing conditions under the assumption of a reasonable coverage of AsH<sub>x</sub> at step edges.

\*Author to whom correspondence should be addressed.

URL: <http://www.ims.tsukuba.ac.jp/lab/shigekawa.index.html>

Electronic address: hata@mat.ims.tsukuba.ac.jp

<sup>1</sup>K. Hata, H. Shigekawa, T. Ueda, M. Akiyama, and T. Okano, *Phys. Rev. B* **55**, 7039 (1997), and references therein.

<sup>2</sup>M. Kasu and N. Kobayashi, *Appl. Phys. Lett.* **62**, 1262 (1993).

<sup>3</sup>K. Ohkuri, J. Ishizaki, S. Hara, and T. Fukui, *J. Cryst. Growth* **160**, 235 (1996).

<sup>4</sup>J. Ishizaki, K. Ohkuri, and T. Fukui, *Jpn. J. Appl. Phys., Part 1* **35**, 1280 (1996).

<sup>5</sup>M. Kasu and N. Kobayashi, *Jpn. J. Appl. Phys., Part 1* **78**, 3026 (1995).

<sup>6</sup>M. Shinohara and N. Inoue, *Appl. Phys. Lett.* **66**, 1936 (1995).

<sup>7</sup>H. Saito, K. Uwai, and N. Kobayashi, *Jpn. J. Appl. Phys., Part 2* **32**, 4400 (1993).

<sup>8</sup>K. Hata, A. Kawazu, T. Okano, T. Ueda, and M. Akiyama, *Appl. Phys. Lett.* **63**, 1625 (1993).

<sup>9</sup>K. Hata, T. Ikoma, H. Hirakawa, T. Okano, A. Kawazu, T. Ueda, and M. Akiyama, *J. Appl. Phys.* **76**, 5601 (1994).

<sup>10</sup>T. Fukui, J. Ishizaki, S. Hara, J. Motohisa, and H. Hasegawa, *J. Cryst. Growth* **146**, 183 (1995).

<sup>11</sup>G. W. Smith, A. J. Pidduck, C. R. Whitehouse, J. L. Glasper, A. M. Keir, and C. Pickering, *Appl. Phys. Lett.* **59**, 3282 (1991).

<sup>12</sup>H. Saito, K. Uwai, and N. Kobayashi, *Jpn. J. Appl. Phys., Part 2* **32**, L4400 (1993).

<sup>13</sup>I. Kamiya, D. E. Aspnes, H. Tanaka, L. T. Florez, J. P. Harrison, and R. Bhat, *Phys. Rev. Lett.* **68**, 627 (1992).

<sup>14</sup>M. D. Pashley, K. W. Haberern, and J. M. Gaines, *Appl. Phys. Lett.* **58**, 406 (1991).

<sup>15</sup>K. Hata, H. Shigekawa, T. Ueda, M. Akiyama, and T. Okano, *J. Vac. Sci. Technol. A* **15**, 1269 (1997).

<sup>16</sup>R. L. Schwoebel and E. J. Shipsey, *J. Appl. Phys.* **37**, 3682 (1966).

<sup>17</sup>G. S. Bales and A. Zangwill, *Phys. Rev. B* **41**, 5500 (1990).

<sup>18</sup>M. D. Pashley, K. W. Haberern, and J. M. Gaines, *Surf. Sci.* **267**, 153 (1992).

<sup>19</sup>J. M. Rickman and D. J. Srolovitz, *Surf. Sci.* **248**, 211 (1993).

<sup>20</sup>E. D. Williams and N. C. Bartelt, *Science* **251**, 393 (1991).

<sup>21</sup>K. Hata *et al.* (unpublished).

<sup>22</sup>J-Sik Lee, S. Iwai, H. Isshiki, T. Meguro, T. Sugano, and Y. Aoyagi, *Appl. Phys. Lett.* **67**, 1283 (1995).

<sup>23</sup>G. Brocks, P. J. Kelly, and R. Car, *Phys. Rev. Lett.* **66**, 1729 (1991).

<sup>24</sup>K. Shiraiishi, *Appl. Phys. Lett.* **60**, 1363 (1992).

<sup>25</sup>C. Chonglin and T. T. Tsong, *Phys. Rev. Lett.* **64**, 3147 (1990).

<sup>26</sup>D. C. Senft and G. Ehrlich, *Phys. Rev. Lett.* **74**, 294 (1995).

<sup>27</sup>S. Kodiyalam, K. E. Khor, and S. Das Sarma, *Phys. Rev. B* **53**, 9913 (1996).

<sup>28</sup>B. S. Swartzentruber and M. Schacht, *Surf. Sci.* **322**, 83 (1995).

<sup>29</sup>T. Shitara, D. D. Vvedensky, M. R. Wilby, J. Zhang, J. H. Neave, and B. A. Joyce, *Phys. Rev. B* **46**, 6825 (1992).

<sup>30</sup>C. Herring, *Phys. Rev.* **82**, 87 (1951).

<sup>31</sup>F. C. Frank, in *Growth and Perfection of Crystals*, edited by R. Doremus, B. Roberts, and D. Turnbull (Wiley, New York, 1958), p. 411.

<sup>32</sup>A. V. Latyshev, A. L. Aseev, A. B. Krasilnikov, and S. I. Stenin, *Surf. Sci.* **213**, 157 (1989).

<sup>33</sup>J. S. Ozcomert, W. W. Pai, N. C. Bartelt, and J. E. Reutt-Robey, *Surf. Sci.* **293**, 183 (1993).